

Compact Branch-Line Coupler with Harmonic Suppression Based on a Planar Simplified Dual Composite Right/Left-Handed Transmission Line Structure

Cheng Wang¹ and Wanchun Tang^{2, 3, *}

Abstract—In this paper, a planar simplified dual composite right/left-handed (SD-CRLH) transmission line (TL) structure is proposed and applied to the design of branch-line coupler. The SD-CRLH TL is obtained by a microstrip line with an open-ended stub in square spiral form. Since this structure has unusual phase shift characteristics with a transmission zero out of the passband, the branch-line coupler with the planar SD-CRLH TL can achieve both size reduction and harmonic suppression. Such a branch-line coupler operating at 0.915 GHz is investigated and fabricated. The equivalent circuit simulation, full-wave simulation and measurement results agree well with each other. From the results, it is shown that the area of the proposed branch line coupler is reduced by 74% compared to the conventional one while maintaining similar performance, and the second harmonic suppression can be lower than -45 dB.

1. INTRODUCTION

Branch-line coupler is an important passive component in practical microwave circuits, which is commonly used in the design of mixers, balanced amplifiers and power dividers, etc. [1]. A conventional branch-line coupler is formed by four quarter-wavelength transmission lines (TLs). At the operating frequency band, it offers equal magnitude and a 90° phase difference in the outputs of the through and coupled ports. However, the conventional branch-line coupler will occupy large area especially at interest low frequency band. Therefore, various techniques have been proposed to miniaturize the size of the branch-line coupler [2–12]. In [2], the size of the coupler can be reduced significantly using lumped elements, but the lumped elements with precise value and high quality are not always available. Then structures employing purely distributed elements are presented to replace the quarter-wavelength TLs. Most of them are realized by different forms of shunt loading, such as low or high impedance lines [3–6], interdigitated capacitor [7]. Other approaches using defected ground structures (DGS) [8, 9], fractal geometries [10, 11], coupled lines [12] are also introduced to effectively reduce the area. However, in some cases, the electrical performance deteriorates compared to the conventional one.

In 2003, the team of Itoh firstly discussed the fundamental properties of composite right/left-hand (CRLH) TL structures [13] Then various physical realizations of 1- and 2-D CRLH TL structures [14–21] were described to demonstrate the practicality in the field of microwave and optical engineering. Caloz proposed the dual composite right/left-hand (D-CRLH) TL structure [22] in 2006, which consists of a parallel LC tank in series and a series (instead of parallel) LC tank in shunt. Compared with CRLH TL structure, D-CRLH TL structure has a stopband between RH and LH passbands with transmission zeros. By taking away a capacitor or an inductor from the LC tank in series or parallel of the D-CRLH

Received 27 February 2018, Accepted 28 May 2018, Scheduled 13 June 2018

* Corresponding author: Wanchun Tang (eewctang@njnu.edu.cn).

¹ School of Electronic and Optical Engineering, Nanjing University of Science and Technology, Nanjing 210094, P. R. China. ² Jiangsu Key Laboratory on Opto-Electronic Technology, Nanjing Normal University, Nanjing 210023, P. R. China. ³ Jiangsu Center for Collaborative Innovation in Geographical Information Resource Development and Application, Nanjing 210023, P. R. China.

TL structure, simplified dual composite right/left-handed (SD-CRLH) TL structures are presented [23], which can reduce both the size and the complexity.

In this paper, a branch-line coupler based on a planar SD-CRLH TL structure is introduced. The planar SD-CRLH TL unit cell is realized by a microstrip line with an open-ended stub in square spiral form. Based on the equivalent circuit analysis, the planar SD-CRLH TL has unusual phase shift characteristics with a transmission zero out of the passband, which can achieve both size reduction and harmonic suppression. Using this planar SD-CRLH TL structure, a branch-line coupler operating at 0.915 GHz is investigated and fabricated. From the results, it can be found that the proposed branch-line coupler reduces the area to 26% of the conventional one while maintaining similar performance, and achieves high second harmonic suppression performance.

2. BASIC THEORY OF THE PLANAR SD-CRLH TL UNIT CELL

A planar SD-CRLH TL unit cell is presented in Fig. 1. It is realized by a microstrip line with an open-ended stub in square spiral form on the substrate, where the square spiral structure is at the center of the microstrip line. The relative permittivity and height of the substrate are ϵ_r and h , respectively. The square spiral structure is completely specified by the number of turns N_s , the turn width w , the turn spacing s , and any one of following: the effective outer dimension d_{out} , or the effective inner dimension d_{in} . An additional TL of length l and width w connected to the microstrip line is also a part of the spiral structure. The length and width of the microstrip line are l_1 and w_1 , respectively. The corresponding equivalent circuit model is established and depicted in Fig. 2, where L_R and L_L correspond to the inductance of the microstrip line L_M and the spiral structure L_S . C is composed by two parts, one is

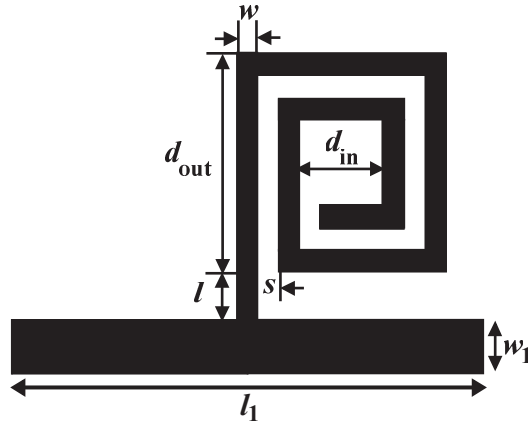


Figure 1. The configuration of the planar SD-CRLH TL unit cell.

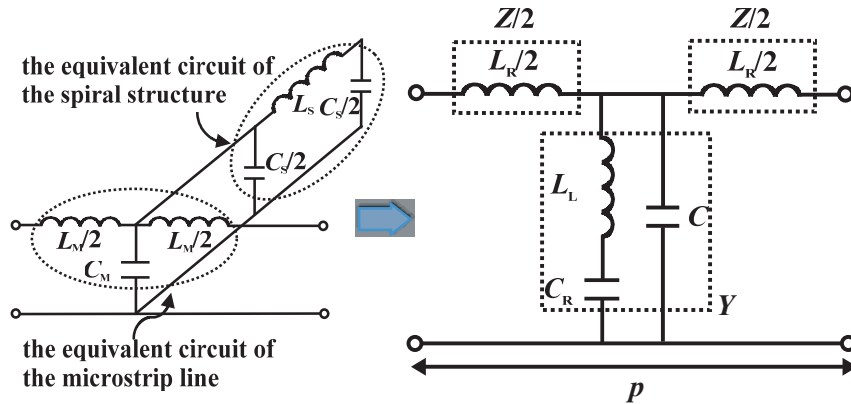


Figure 2. The equivalent circuit of the planar SD-CRLH TL unit cell.

the capacitance between the microstrip line and ground, and another is the capacitance between the open-ended stub in spiral form and ground, i.e., $C_M + C_S/2$, while C_R is denoted by $C_S/2$. So C is larger than C_R . Compared with the conventional D-CRLH TL structure, the proposed SD-CRLH TL structure takes away a capacitor (C_L) from the LC tank in series.

The transmission matrix of the planar SD-CRLH TL unit cell can be written as

$$\begin{aligned} \begin{bmatrix} A & B \\ C & D \end{bmatrix} &= \begin{bmatrix} 1 & \frac{Z}{2} \\ 0 & 1 \end{bmatrix} \begin{bmatrix} 1 & 0 \\ Y & 1 \end{bmatrix} \begin{bmatrix} 1 & \frac{Z}{2} \\ 0 & 1 \end{bmatrix} \\ &= \begin{bmatrix} 1 + \frac{ZY}{2} & Z(1 + \frac{ZY}{4}) \\ Y & 1 + \frac{ZY}{2} \end{bmatrix} \end{aligned} \quad (1)$$

where the impedance Z and the admittance Y are, respectively,

$$Z = j\omega L_R \quad (2)$$

$$Y = j\omega \left(C + \frac{C_R}{1 - \omega^2 L_L C_R} \right) \quad (3)$$

One may note that this SD-CRLH TL unit cell has a transmission zero at

$$\omega_z = \sqrt{\frac{1}{L_L C_R}} \quad (4)$$

On the basis of the periodic boundary condition (PBCs) and the Bloch-Floquet theorem [1], the dispersion equation and the Bloch impedance are as follows:

$$\begin{aligned} \gamma(\omega) = \alpha(\omega) + j\beta(\omega) &= \frac{1}{p} \cosh^{-1} \left(\frac{A + D}{2} \right) \\ &= \frac{1}{p} \cosh^{-1} \left(1 - \omega^2 \frac{L_R}{2} \left(C + \frac{C_R}{1 - \omega^2 L_L C_R} \right) \right) \end{aligned} \quad (5)$$

$$\begin{aligned} Z_B(\omega) &= \frac{B}{\sqrt{A^2 - 1}} \\ &= \sqrt{L_R \left(1 - \omega^2 \frac{L_R}{4} \left(C + \frac{C_R}{1 - \omega^2 L_L C_R} \right) \right) / \left(C + \frac{C_R}{1 - \omega^2 L_L C_R} \right)} \end{aligned} \quad (6)$$

where $\gamma(\omega)$ is the complex propagation constant with the attenuation constant $\alpha(\omega)$ and the phase constant $\beta(\omega)$. And p is the length of the SD-CRLH TL unit cell which is less than $\lambda_g/4$, where λ_g represents the guided wavelength.

From Eq. (5), we can find that the wave can propagate only when $|(A + D)/2| < 1$, that is

$$-4 < ZY < 0 \quad (7)$$

Substituting Eqs. (2) and (3) into Eq. (7), we obtain the condition of the wave which can propagate,

$$0 < \omega < \omega_1, \quad \omega_2 < \omega < \omega_3 \quad (8)$$

with $\omega_1 = \sqrt{\frac{L_R C + L_R C_R + 4L_L C_R - \sqrt{(L_R C + L_R C_R + 4L_L C_R)^2 - 16L_L C_R L_R C}}{2L_L C_R L_R C}}$, $\omega_2 = \sqrt{(1 + \frac{C_R}{C}) \frac{1}{L_L C_R}}$, and $\omega_3 = \sqrt{\frac{L_R C + L_R C_R + 4L_L C_R + \sqrt{(L_R C + L_R C_R + 4L_L C_R)^2 - 16L_L C_R L_R C}}{2L_L C_R L_R C}}$.

It is obvious that this structure has two passbands, i.e., from 0 to ω_1 and from ω_2 to ω_3 . In addition, the transmission zero ω_z is in the stopband between the two passbands (i.e., $\omega_1 < \omega_z < \omega_2$).

3. BRANCH-LINE COUPLER USING THE PLANAR SD-CRLH TL STRUCTURE

The conventional branch-line coupler is constituted of two pairs of *quarter-wavelength* TLs with characteristic impedances Z_0 and $Z_0/\sqrt{2}$, respectively, as shown in Fig. 3. And each *quarter-wavelength*

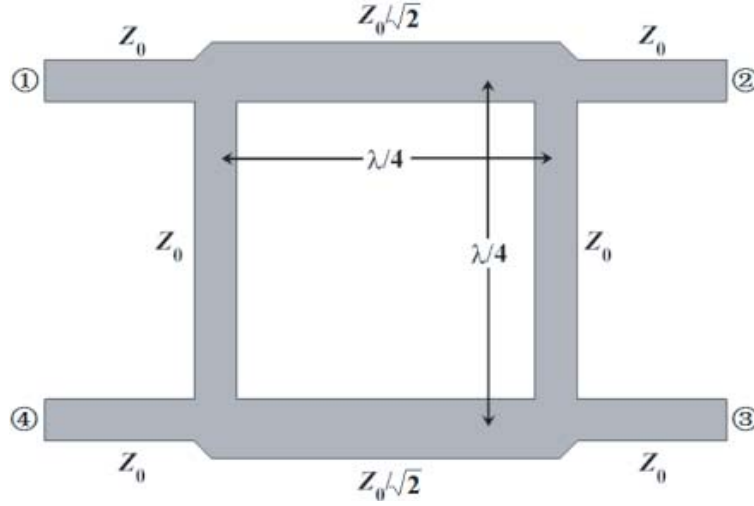


Figure 3. Topology of the conventional branch-line coupler.

TL will be replaced by the proposed planar SD-CRLH TL with N unit cells to realize the miniaturization of the branch-line coupler and suppress its second harmonics.

For the *quarter-wavelength* TLs with $Z_0 = 50 \Omega$, the total phase shift of the planar SD-CRLH TL is $\phi(\omega_0) = N\Delta\phi(\omega_0) = \pi/2$ at the operating frequency of ω_0 , where $\Delta\phi(\omega_0) = \beta(\omega_0)p$ is the phase shift of each planar SD-CRLH TL unit cell, and the *Bloch* impedance $Z_B(\omega_0) = Z_0 = 50 \Omega$. Using the Eqs. (5) and (6), these two conditions can be written as follows:

$$1 - \omega_0^2 \frac{L_R}{2} \left(C + \frac{C_R}{1 - \omega_0^2 L_L C_R} \right) = \cos(\beta(\omega_0)p) = \cos(\pi/2N) \quad (9)$$

$$\sqrt{L_R \left(1 - \omega_0^2 \frac{L_R}{4} \left(C + \frac{C_R}{1 - \omega_0^2 L_L C_R} \right) \right) / \left(C + \frac{C_R}{1 - \omega_0^2 L_L C_R} \right)} = Z_0 \quad (10)$$

The transmission zero of the planar SD-CRLH TL unit cell will be set as twice of the operating frequency, i.e., $\omega_z = 2\omega_0$, so that the second harmonics of the branch-line coupler can be suppressed. And the operating frequency ω_0 is in the first passband.

From the above description and the Eqs. (9) to (10), we can obtain the following expressions for the components in the equivalent circuit model of Fig. 2.

$$L_R = \frac{100}{\omega_0} \sqrt{\frac{1 - \cos(\pi/2N)}{1 + \cos(\pi/2N)}} \quad (11a)$$

$$C + \frac{4C_R}{3} = \frac{1}{50\omega_0} \sqrt{1 - (\cos(\pi/2N))^2} \quad (11b)$$

$$L_L = \frac{1}{4\omega_0^2 C_R} \quad (11c)$$

When ω_0 , N and C_R are determined, using Eqs. (11a)–(11c) the parameters of the equivalent circuit can be calculated. Then the CAD formulas in [24] to calculated equivalent circuit components of the square spiral structure are given as follows:

$$L_S = 4 \frac{\mu_0 \varepsilon_0}{\left(C_{1/4near}^m + C_{1/4far}^m \right)^{1/m}} N_s^2 (b_1 + b_2)^2 \quad (12a)$$

where $m = 1.42(w/w_s)^{0.22}(h/d_{out})^{0.15}$, $C_{1/4near} = \frac{\varepsilon_0 A_{1/4}}{h} \cdot \frac{w}{w_s}$, $C_{1/4far} = \frac{1}{\left[\frac{1}{c_{f1\varepsilon_0} \sqrt{8\pi A_{1/4}}} + \frac{\Delta p_{11} - \Delta p_{110}}{N_s M} \right] - \frac{1}{4\pi\varepsilon_0 r_0}}$,
 $r_0 = \frac{4(b_1^2 + b_1 b_2 + b_2^2)}{3(b_1 + b_2)}$, $c_{f1} = 1.07\left(\frac{b_1}{b_2}\right)^3 - 0.92\left(\frac{b_1}{b_2}\right)^2 + 0.3\left(\frac{b_1}{b_2}\right) + 0.82$, $\Delta p_{11} = \frac{1}{c_{f\varepsilon_0} \sqrt{8\pi w w_s}}$, $\Delta p_{110} = \frac{1}{c_{f\varepsilon_0} \sqrt{8\pi w_s^2}}$, $c_f =$

0.865, $w_s=w+s$, $M=(b_1+b_2)/w_s$, $A_{1/4}=b_2^2 - b_1^2$, $b_1=(d_{in}-s)/2$, $b_2=(d_{out}+s)/2$.

$$C_S = (C_{near}^n + C_{far}^m)^{1/n} \tag{12b}$$

where $C_{near} = \frac{4\epsilon_r\epsilon_0 A_{1/4}}{h} \cdot \frac{w}{w_s}$, $C_{far} = \frac{1}{[\frac{1}{c_{f2}\epsilon_0\sqrt{32\pi A_{1/4}}} + \frac{\Delta P_{11} - \Delta P_{110}}{4N_s M}] \frac{2}{\epsilon_r + 1}}$, $c_{f2} = 0.9(1 - d_{in}/d_{out})^{-0.18}$, $n = 1.114(1 - d_{in}/d_{out})^{0.16}(w/w_s)^{0.31}$. As the inductance and capacitance of the square spiral structure are determined, d_{out} , w , s , d_{in} , and N_s can be fitted to match these values.

Since the characteristic impedance of the microstrip line is $Z_0 = \sqrt{L_M/C_M}$. Using the formulas in [25], the width w_1 can be calculated as

$$\frac{h}{w_1} = \left\{ \left[Z_0 \sqrt{\frac{\epsilon_0 \epsilon_r}{\mu_0}} \right]^{n1} + \left[\frac{1}{8} \left(e^{2\pi Z_0 \sqrt{\frac{\epsilon_0(\epsilon_r+1)}{2\mu_0}}} - \left(1 + 2\pi Z_0 \sqrt{\frac{\epsilon_0(\epsilon_r+1)}{2\mu_0}} \right) \right) \right]^{n1} \right\}^{1/n1} \tag{13a}$$

where $n1 = 0.911 - 0.00629\epsilon_r$. The capacitance C_m of per unit length microstrip line is

$$C_m = \left\{ \left[\frac{\epsilon_0 \epsilon_r w_1}{h} \right]^q + \left[2\pi \epsilon_0 \frac{\epsilon_r + 1}{2} \left(\frac{1}{\ln(8h/w_1 + 1)} - \frac{w_1}{8h} \right) \right]^q \right\}^{1/q} \tag{13b}$$

where $q = 1.07$. And the length l_1 is obtained as C_M/C_m .

- Briefly, the design procedure of the planar SD-CRLH TL unit cell can be summarized as follows:
- Step 1) Determine the operating frequency ω_0 and the number of the planar SD-CRLH TL unit cells N .
 - Step 2) Choose a suitable value for C_R .
 - Step 3) Use Eq. (11) to calculate the other values of the equivalent circuit L_R , L_L , and C .
 - Step 4) For the values of C_R and L_L , apply the Eqs. (12)–(13) to determine l , d_{out} , w , s , d_{in} , and N_s .
 - Step 5) Use the Eqs. (13a)–(13b) and determined values of L_R and $C - C_R$ in order to obtain w_1 and l_1 of Fig. 1.

As an example, the operating frequency of the proposed branch-line coupler is chosen as 0.915 GHz, and it is fabricated on a 32-mil Rogers RO4003C substrate. Then N should be selected properly. Here, $N = 1, 3$, and 5 are considered, since C_R should be less than C , according to Eq. (11b), C_R is less than 1.49 pF, 0.74 pF, and 0.46 pF, respectively. For comparison, C_R is taken as 0.35 pF. Using the above design steps (1)–(5), the dimensions of the planar SD-CRLH TL unit cell with different N are given in Table 1. In Fig. 4, the S -parameters of the planar SD-CRLH TL with different N by both the equivalent circuit simulation and the full-wave simulation are illustrated. The total phase shift and the Bloch impedance of the planar SD-CRLH TL with different N by the full-wave simulation are shown in Fig. 5 and Fig. 6, respectively. From the results in Fig. 4, it is shown that when $N = 1$, the frequency characteristics do not agree well with the results of the equivalent circuit simulation, and the total phase shift $\phi(\omega_0)$ and Bloch impedance $Z_B(\omega_0)$ in Figs. 5 and 6 are also not accurate at 0.915 GHz. The reason is that the calculated characteristic impedance of the microstrip line is $Z_0 = \sqrt{L_M/C_M}$, which means that the equivalent circuit is only suitable at low frequency range. When using one proposed unit cell to replace the conventional *quarter-wavelength* microstrip line, it is found that the length of

Table 1. The dimensions of the planar SD-CRLH TL unit cell (unit: mm).

N	w_1	l_1	l	d_{out}	w	s	d_{in}	N_s
1	0.63	35.4	0.8	3.8	0.3	0.2	1.2	3
3	0.9	11.2	0.8	3.8	0.3	0.2	1.2	3
5	0.34	4.4	0.8	3.8	0.3	0.2	1.2	3

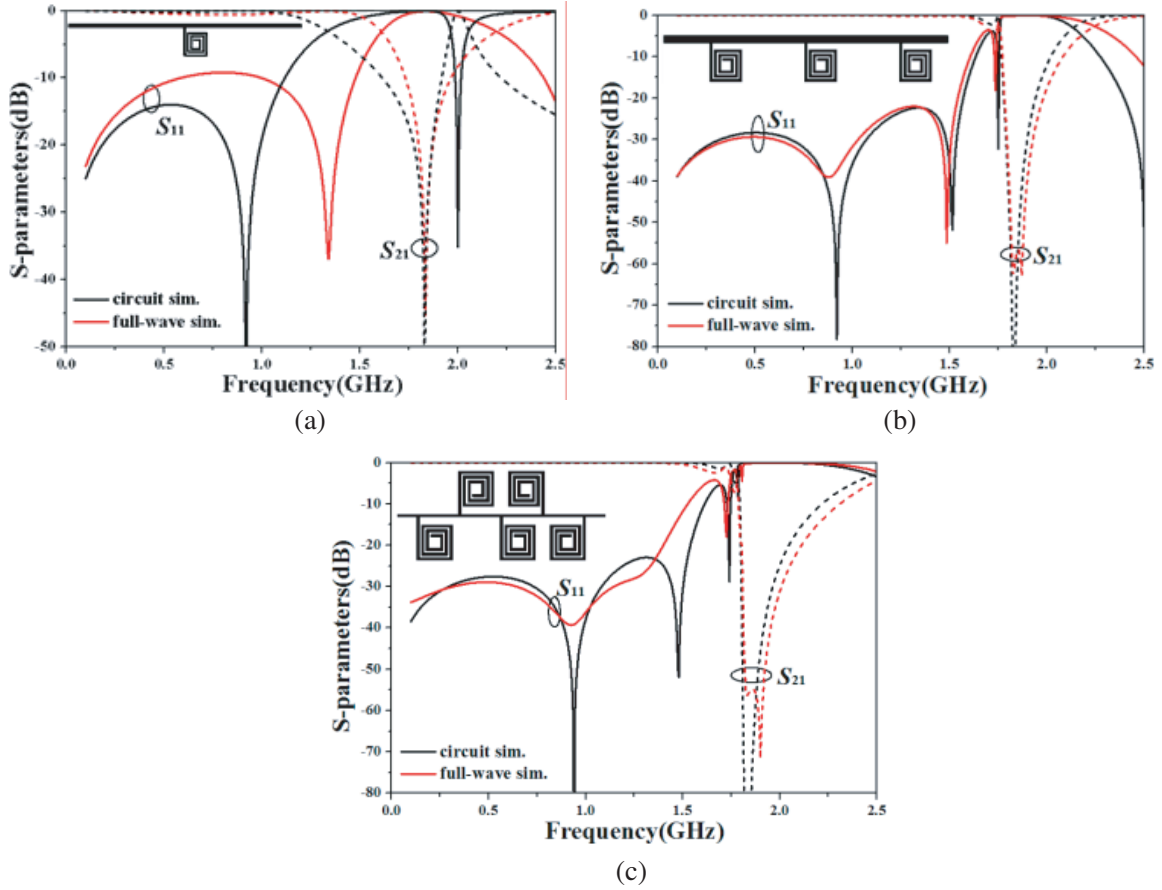


Figure 4. S -parameters of the planar SD-CRLH TLs with different N . (a) $N = 1$, (b) $N = 3$, (c) $N = 5$.

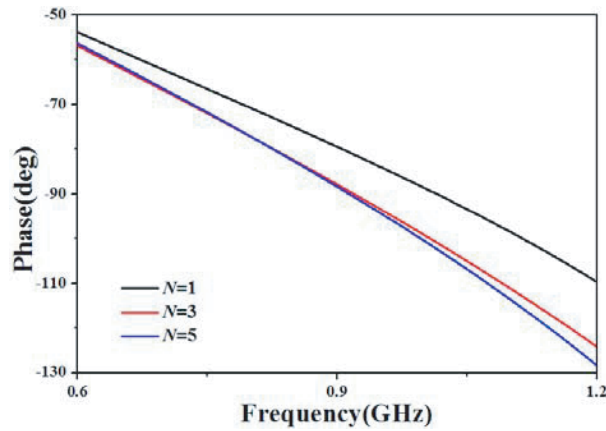


Figure 5. The total phase shift of the planar SD-CRLH TLs with different N by the full-wave simulation.

the microstrip line is not small enough, then the method in [25] to obtain w_1 and l_1 is not effective. For $N = 3$ or $N = 5$, the frequency characteristics are similar between the equivalent circuit and full wave simulation in Fig. 4. From Figs. 5 and 6, it is observed that the planar SD-CRLH TLs have the total phase shift $\phi(\omega_0) = \pi/2$ and the Bloch impedance $Z_B(\omega_0) = 50 \Omega$ at 0.915 GHz. What's more, the total phase shift $\phi(\omega)$ with $N = 3$ or $N = 5$ is nearly linear and the Bloch impedance $Z_B(\omega)$ is almost

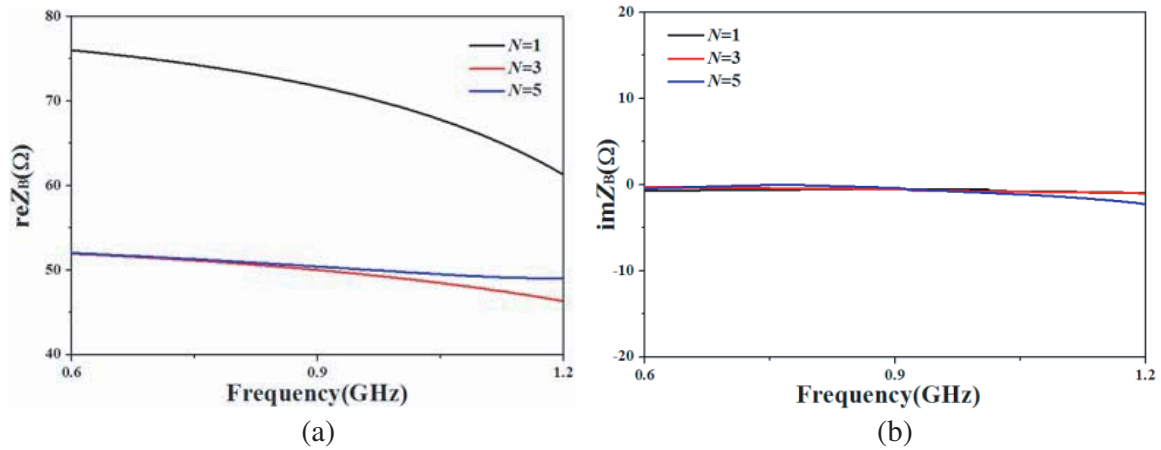


Figure 6. The Bloch impedance of the planar SD-CRLH TLs with different N by the full-wave simulation. (a) reZ_B , (b) imZ_B .

frequency independent from 0.6 GHz to 1.2 GHz, which mean that both the planar SD-CRLH TLs with $N = 3$ and $N = 5$ can replace the conventional *quarter-wavelength* microstrip line. While for $N = 5$, the planar SD-CRLH TL unit cells cannot arrange in the same side from Fig. 4(c), which will go against miniaturization of the branch-line coupler. So, $N = 3$ is a suitable choice in this design. The total length of the planar SD-CRLH TL with $N = 3$ is 33.6 mm, while the conventional *quarter-wavelength* microstrip line is 50.1 mm at 0.915 GHz, which means the proposed structure can achieve size reduction. At 1.83 GHz, S_{21} is -63 dB, the second harmonics are suppressed significantly.

Similarly, for the other *quarter-wavelength* TLs with $Z_0/\sqrt{2} = 35.4 \Omega$ each TL is also replaced by 3 planar SD-CRLH TL unit cells. The equivalent circuit values are $L_R = 3.29$ nH, $L_L = 15.12$ nH, $C_R = 0.5$ pF, and $C = 1.79$ pF. The dimensions of the planar SD-CRLH TL unit cell are calculated as follows: $w_1 = 1.75$ mm, $l_1 = 10.8$ mm, $l = 1.1$ mm, $d_{out} = 4.7$ mm, $w = 0.5$ mm, $s = 0.3$ mm, $d_{in} = 2.1$ mm, and $N_s = 2$.

4. EXPERIMENTAL RESULTS

For experimental validation, the proposed branch-line coupler is fabricated, and its configuration is illustrated in Fig. 7. In order to make the proposed coupler more compact, one planar SD-CRLH TL unit cell is folded. The measured S -parameters are given in Fig. 8. For comparison, the equivalent circuit and the full-wave simulation results are also added. It can be seen that all results achieve good agreements. What's more, it also can be observed that in the frequency range of 0.79–1.04 GHz, the

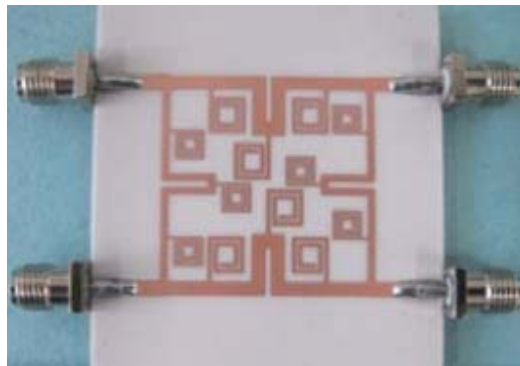


Figure 7. Photograph of the designed branch-line coupler.

return loss and isolation are lower than -10 dB. At 0.915 GHz, the measured insertion loss $|S_{21}|$ and $|S_{31}|$ are -3 dB, -3.32 dB, respectively. And the second harmonic signals are significantly suppressed with $|S_{21}|$ and $|S_{31}|$ under -45 dB at 1.83 GHz. Fig. 9 shows the phase difference and amplitude balance between $|S_{21}|$ and $|S_{31}|$. For phase difference within $90^\circ \pm 2^\circ$, the frequency range is from 0.8 to 1.05 GHz, while amplitude balance varies from -1.51 to 0.35 dB. In addition, the dimension of the fabricated prototype shown in Fig. 7 is $25.8 \text{ mm} \times 25 \text{ mm}$ ($0.13\lambda_g \times 0.125\lambda_g$), where λ_g is the guided wavelength at the operating frequency), which shows an area reduction of 74% compared with the conventional branch-line coupler. In Table 2, the performance of both the proposed and conventional branch-line coupler are summarized, it is shown that the performance of the proposed coupler is similar with the conventional one, while it can significantly reduce the size and get the harmonic suppression.

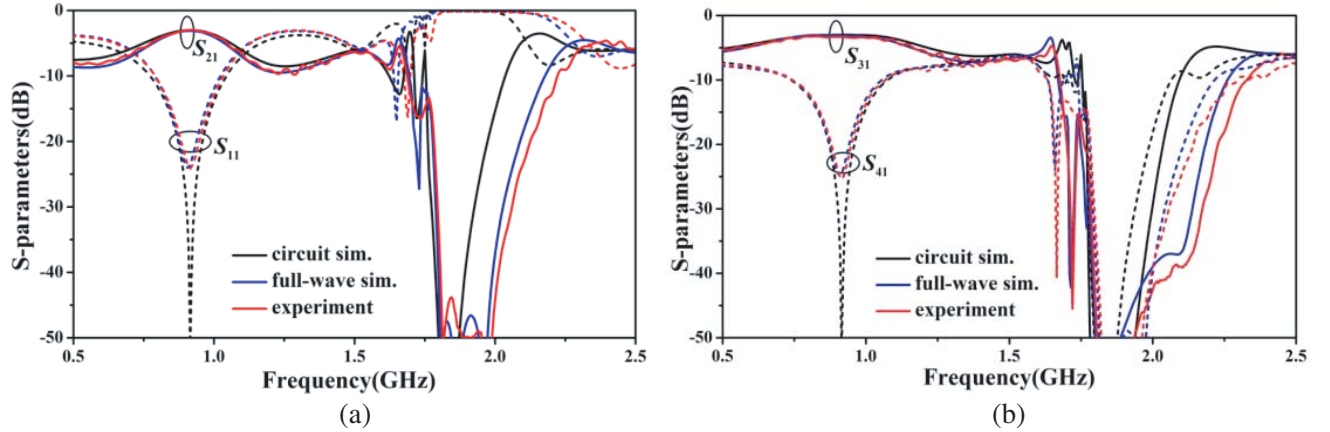


Figure 8. S -parameters of the proposed branch-line coupler. (a) $|S_{11}|$ (dash lines), $|S_{21}|$ (solid lines), (b) $|S_{31}|$ (solid lines), $|S_{41}|$ (dash lines).

Table 2. Comparison of conventional and proposed branch-line couplers.

	Conventional	Proposed
Reactive area	100%	26%
Insertion loss $ S_{21} $, $ S_{31} $ (dB)	-3.33 , -2.98	-3 , -3.32
Return loss $ S_{11} $ (dB)	-23.4	-24.2
Isolation $ S_{41} $ (dB)	-25.5	-25.3
Phase difference	89.7°	89.7°
Harmonic suppression	No	Yes

Table 3. Comparison of previous and proposed branch-line couplers.

Ref.	Technology	Reactive area	Harmonic suppression
[4]	Distributed Capacitors	38%	Not shown
[5]	Asymmetrical T-Structures	12.2%	Not shown
[6]	H-shaped transmission lines	36%	Yes
[7]	Interdigitated shunt capacitors	26.8%	Yes
[9]	CSRRs	40%	Not shown
[11]	Symmetric polygonal folding lines	24%	Not shown
[12]	Coupled lines	33%	Not shown
This work	planar SD-CRLH TLs	26%	Yes

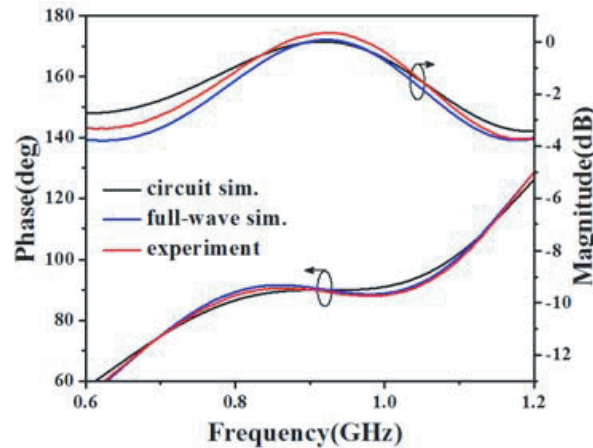


Figure 9. Phase difference and amplitude balance between S_{21} and S_{31} of the proposed branch-line coupler.

Table 3 summarizes the comparison of the proposed coupler with others in previous literatures. From the table it is found that the proposed branch-line coupler has good performance.

5. CONCLUSION

In this paper, a branch-line coupler based on a planar SD-CRLH TL structure is presented. Compared to the conventional microstrip line, the proposed planar SD-CRLH TL has unusual phase shift characteristics with a transmission zero out of the passband. With this structure, a branch-line coupler is investigated and fabricated, and the design procedure is also presented. From the results, the proposed branch-line coupler effectively reduces the area compared to the conventional one while maintaining approximately the same performance, and has high second harmonic suppression performance. With these good features, it is applicable to microwave system applications.

ACKNOWLEDGMENT

This work was supported by the National Natural Science Foundation of China (Grant No. 61571232), and the Research Innovation Program for College Graduates of Jiangsu Province (Grant No. KYLX16{1291}).

REFERENCES

1. Pozar, D. M., *Microwave Engineering*, John Wiley & Sons, New York, 2005.
2. Vogel, R. W., "Analysis and design of lumped-and lumped-distributed-element directional couplers for MIC and MMIC applications," *IEEE Trans. Microw. Theory Tech.*, Vol. 40, No. 2, 253–262, Feb. 1992.
3. Tang, C. W. and M. G. Chen, "Synthesizing microstrip branch-line couplers with predetermined compact size and bandwidth," *IEEE Trans. Microw. Theory Tech.*, Vol. 55, No. 9, 1926–1934, Sep. 2007.
4. Jung, S. C., R. Negra, and F. M. Ghannouchi, "A design methodology for miniaturized 3-dB branch-Line hybrid couplers using distributed capacitors printed in the inner area," *IEEE Trans. Microw. Theory Tech.*, Vol. 56, No. 12, 2950–2953, Dec. 2008.
5. Tseng, C. H. and C. L. Chang, "A rigorous design methodology for compact planar branch-line and rat-race couplers with asymmetrical T-structures," *IEEE Trans. Microw. Theory Tech.*, Vol. 60, No. 7, 2085–2092, Jul. 2012.

6. Krishna, I. S., R. K. Barik, S. S. Karthikeyan, and P. Kokil, "A miniaturized harmonic suppressed 3 dB branch line coupler using H-shaped microstrip line," *Microw. and Opt. Technol. Lett.*, Vol. 59, No. 4, 913–918, 2017.
7. Tsai, K.-Y. H.-S. Yang, J.-H. Chen, and Y.-J. E. Chen, "A miniaturized 3 dB branch-line hybrid coupler with harmonics suppression," *IEEE Microw. Wirel. Compon. Lett.*, Vol. 21, 537–539, 2011.
8. Dwari, S. and S. Sanyal, "Size reduction and harmonic suppression of microstrip branch-line coupler using defected ground structure," *Microw. and Opt. Technol. Lett.*, Vol. 48, No. 10, 1966–1969, 2006.
9. Savitri, B., V. A. Fono, B. Alavikia, L. Talbi, and K. Hettak, "Novel approach in design of miniaturized passive microwave circuit components using metamaterials," *Microw. and Opt. Technol. Lett.*, Vol. 59, No. 6, 1341–1347, 2017.
10. Ghali, H. and T. A. Moselhy, "Miniaturized fractal rat-race, branch-line, and coupled-line hybrids," *IEEE Trans. Microw. Theory Tech.*, Vol. 52, No. 11, 2513–2520, Nov. 2004.
11. Velan, S. and M. Kanagasabai, "Compact microstrip branch-line coupler mwith wideband quadrature phase balance," *Microw. and Opt. Technol. Lett.*, Vol. 58, No. 6, 1369–1374, 2016.
12. Reshma, S. and M. K. Mandal, "Miniaturization of a 90° hybrid coupler with improved bandwidth performance," *IEEE Microw. Wirel. Compon. Lett.*, Vol. 26, 891–893, 2016.
13. Lai, A., T. Itoh, and C. Caloz, "Composite right/left-handed transmission line metamaterials," *IEEE Microw. Mag.*, Vol. 5, No. 3, 34–50, 2004.
14. Yang, T., P. L. Chi, and T. Itoh, "Compact quarter-wave resonator and its applications to miniaturized diplexer and triplexer," *IEEE Trans. Microw. Theory Tech.*, Vol. 59, No. 2, 260–269, Feb. 2011.
15. Xu, H. X., G. M. Wang, Z. M. Xu, et al., "Dual-shunt branch circuit and harmonic suppressed device application," *Appl. Phys. A*, Vol. 108, No. 2, 497–502, 2012.
16. Xu, H. X., G. M. Wang, X. Chen, and T. P. Li, "Broadband balun using fully artificial fractal-shaped composite right/left handed transmission line," *IEEE Microw. Wirel. Compon. Lett.*, Vol. 22, No. 1, 16–18, 2012.
17. Caloz, C., T. Itoh, and A. Rennings, "CRLH metamaterial leaky-wave and resonant antennas," *IEEE Antennas Propag. Mag.*, Vol. 50, No. 5, 25–39, 2008.
18. Xu, H. X., G. M. Wang, M. Q. Qi, et al., "Analysis and design of two-dimensional resonant-type composite right left handed transmission lines with compact gain-enhanced resonant antennas," *IEEE Trans. Antennas Propag.*, Vol. 61, No. 2, 735–747, 2013.
19. Xu, H. X., G. M. Wang, M. Q. Qi, and T. Cai, "Compact fractal left-handed structures for improved cross-polarization radiation pattern," *IEEE Trans. Antennas Propag.*, Vol. 62, No. 2, 546–554, 2014.
20. Iyer, A. K. and G. V. Eleftheriades, "Free-space imaging beyond the diffraction limit using a Veselago-Pendry transmission-line metamaterial superlens," *IEEE Trans. Antennas Propag.*, Vol. 57, No. 6, 1720–1727, 2009.
21. Xu, H. X., G. M. Wang, M. Q. Qi, et al., "Metamaterial lens made of fully printed resonant-type negative-refractive index transmission lines," *Appl. Phys. Lett.*, Vol. 102, 193502, 2013.
22. Caloz, C., "Dual Composite Right/Left-Handed (D-CRLH) transmission line metamaterial," *IEEE Microw. Wirel. Compon. Lett.*, Vol. 16, 585–587, 2006.
23. Wang, C., Y. R. Shi, S. Liu, et al., "Ultra-wideband bandpass filter using simplified dual composite right/left-handed transmission line structure," *Microw. and Opt. Technol. Lett.*, Vol. 55, No. 5, 1165–1167, 2013.
24. Tang, W., X. He, T. Pan, and Y. L. Chow, "Synthetic asymptote formulas of equivalent circuit components of square spiral inductors," *Journal of Electromagnetic Waves and Applications*, Vol. 20, No. 2, 215–226, 2006.
25. Chow, Y. L. and W. C. Tang, "Development of CAD formulas of integrated circuit components-fuzzy EM formulation followed by rigorous derivation," *Journal of Electromagnetic Waves and Applications*, Vol. 15, No. 8, 1097–1119, 2001.